The Mechanism of Vanadium-Mediated Developmental Hypomyelination Is Related to Destruction of Oligodendrocyte Progenitors Through a Relationship with Ferritin and Iron

Bozho Todorich · James O. Olopade · Nodar Surguladze · Xuesheng Zhang · Elizabeth Neely · James R. Connor

Abstract The second post-natal week in rat is the period of the most intense oligodendrocyte development and myelination. This period coincides with peak iron import by oligodendrocytes. During that time oligodendrocyte progenitors (OPCs) are sensitive to agents that may disturb normal iron homeostasis and assimilation of iron into these cells. One mechanism by which iron homeostasis can be disrupted is by environmental exposure to other metals. Vanadium is a transition metal, and exposure to vanadium during early brain development produces hypomyelination with variety of related neuro-behavioral phenotypes. In the current study, we investigated mechanisms of hypomyelination induced by vanadium exposure in developing rat brain. We demonstrate that both in vivo and in vitro, OPCs are more sensitive to vanadium exposure than astrocytes or mature oligodendrocytes. Vanadium exposure in OPCs resulted in increased ROS generation and increased annexinV labeling suggestive of apoptosis. Because ferritin is a major iron delivery protein for oligodendrocytes, we exposed the cells to recombinant ferritin and iron both of which exacerbated vanadium cytotoxicity, while the iron chelator desferroxamine (DFO) prevented cytotoxic/apoptotic effects of vanadium. To illustrate relationship between ferritin and vanadium, we demonstrate that vanadium exacerbated DNA nicking produced by iron-rich spleen ferritin, but not iron-poor apoferritin, resulting in a single and double strand breaks in a DNA relaxation assay. We propose that developmental exposure to vanadium interferes with normal iron assimilation into oligodendrocytes resulting in oxidative stress and apoptosis. Therefore, depletion of OPCs due to vanadium exposure in early post-natal period may be an important mechanism of vanadium-induced hypomyelination.

Keywords Vanadium · Iron · Ferritin · Oligodendrocytes · Myelination · Development

Abbreviations
OPCs	Oligodendrocyte progenitor cells
ROS	Reactive oxygen species
DFO	Desferroxamine
Fe	Iron
V	Vanadium
H_2O_2	Hydrogen peroxide

B. Todorich · J. O. Olopade · N. Surguladze · X. Zhang · E. Neely · J. R. Connor (✉)
Department of Neurosurgery (H110), Pennsylvania State University College of Medicine, M.S. Hershey Medical Center, 500 University Drive, Hershey, PA 17033-0850, USA
e-mail: jconnor@psu.edu; jrc3@psu.edu

J. O. Olopade
Department of Veterinary Anatomy, University of Ibadan, Ibadan, Nigeria

N. Surguladze
Institute of Molecular Biology and Biological Physics, 12 Gotua St., 0160 Tbilisi, Georgia

Introduction

Vanadium is a metal in the first transition series and it is widely distributed in nature (Nriagu and Pacyna 1988). While some derivatives of vanadium have been found useful in medicine and industry (Ray et al. 2006), acute environmental and occupational exposure to this metal

continues to be a health risk to humans and animals (Shrivastava 2007). Vanadium emission from human industrial activities has been estimated to comprise about 53% of total atmospheric vanadium (Hope 1994). A major source of vanadium toxicity remains the burning of fossil fuels in the Arabian Gulf (Haider et al. 1998) and the Niger Delta region of Nigeria (Igado et al. 2008) where massive incidental and or intentional burning of vanadium containing fuels results in pollution of confined ecosystems.

Little is known about tissue and cellular mechanisms of vanadium toxicity. Current opinion is that vanadium induces oxidative stress caused by free radical generation and this action has been strongly linked to the majority of the toxic and molecular effects of vanadium compounds on biological systems (Evangelou 2002). Antioxidants such as vitamin E (α-tocopherol) and its derivatives, ascorbic acid and catalase, directly or indirectly protect cells against adverse effects of toxic radical reactions resulting from vanadium exposure (Mates 2000). Vanadium at the +5 oxidative state (metavanadate) entering the biological system is reduced to vanadyl (IV) by glutathione in erythrocytes or by ascorbic acid and other reducing substances in plasma and then transported by albumin and transferrin, a major iron transport protein (Sabbioni and Marafante 1981; Degani et al. 1981). At the cellular level, vanadium (V) enters the cell through anion transport mechanisms (Heinz et al. 1982) and/or the transferrin/transferrin receptor system (Nagaoka et al. 2004), and becomes reduced to vanadyl mainly by intracellular glutathione (Sabbioni et al. 1993). Although there is little data in relation to vanadium interactions with iron within biological systems, it is possible that absorbed vanadium is bound in part to transferrin and that vanadium could interfere with the metabolism and storage of iron and vice versa (EVM 2002). A similar mechanism has been proposed for aluminum (Roskams and Connor 1990).

One of the major pathologic effects of vanadium on CNS appears to be myelin disruption (Garcia et al. 2004). Treating adult rats with vanadium results in histological disruption of myelin, which is accompanied by increased lipid peroxidation in discrete brain areas (Garcia et al. 2004; Sasi et al. 1994). Exposure of neonatal rats to sodium metavanadate results in a variety of behavioral defects with motor impairments (Soazo and Garcia 2007). The behavioral alterations were accompanied by and attributed to significant myelin pathology; decreased thickness of corpus callosum and decreased staining of MBP in corpus callosum and cerebellum (Soazo and Garcia 2007). The relevant follow up question to this latter study is the effect of vanadium on oligodendrocytes, the myelin producing cells in the CNS. The answer to this question will be key in developing treatment strategies for vanadium toxicity. We hypothesized that developmental exposure to vanadium causes hypomyelination via destruction of oligodendrocyte progenitors by virtue of interfering with iron assimilation and increasing iron release from ferritin, resulting in oxidative stress and apoptosis of OPCs.

In the current study, we show that vanadium exposure in the early post-natal period results in destruction of oligodendrocyte progenitors, but not astrocytes both in vivo and in vitro. We also demonstrate that vanadium exposure produces a cytotoxic effect on OPCs resulting from increase in oxidative stress and apoptosis of OPCs. Finally we show that vanadium induces release of iron from ferritin and that ferritin and iron exposure exacerbates the cytotoxic effects of vanadium. Considering the established role of ferritin in iron homeostasis of developing oligodendrocytes (Todorich et al. 2009), our findings suggest that high content of iron and ferritin in developing oligodendrocytes make them uniquely vulnerable to vanadium exposure, and that the destruction of OPCs may be the key contributor to vanadium-induced developmental hypomyelination.

Materials and Methods

Reagents

Sodium metavanadate (Sigma) was obtained as powder and diluted with PBS to a stock solution of 2.5 mM, which was kept in aliquots at $-20°C$, and used as needed. Desferroxamine (Sigma) was dissolved in water and frozen in 100 mM aliquots of stock solution, which were used for individual experiments.

Animals

Pregnant Sprague–Dawley rat dams at two weeks of gestation were purchased from Charles River Laboratories, and housed at Pennsylvania State University College of Medicine Animal Core facilities. All experiments on animals were performed in accordance with ethical standards and Institutional animal care and use committee (IACUC, protocol numbers: 98-007; 2008-022). Starting at post-natal day 1 (P1), rat pups ($N = 5$) were injected with 3 mg/kg Na-metavanadate IP once daily for 14 days as reported in Garcia et al. (2004) and Soazo and Garcia (2007)). These concentrations were previously shown to induce hypomyelination in both adult and developing rat pups (Garcia et al. 2004; Soazo and Garcia 2007). Littermate controls ($N = 5$) receiving the same volume of saline were used as controls. The pups were housed with their dams with ad libitum access to food. During the study their weights were measured daily on a benchtop scale. At P15, rotarod testing of motor function was performed on the vanadium-treated and

control rats. Briefly, all animals were taken through a training period on the rotarod, and subsequently tested in three independent trials at a speed of 5 rpms. The outcome was the time it took for the rat to fall off the rotarod. The rotorod performance was scored by two investigators blinded to the experimental condition with good concordance. The times of three trials were averaged across each group and evaluated for statistical significance using unpaired t-test. Subsequently, animals were anesthetized and perfused transcardially with ice-cold PBS (pH = 7.4) for 10 min. Brains were removed and placed in 4% paraformaldehyde for 24 h. Subsequently after a brief rinse in PBS, brains were taken through the sucrose gradient (10, 20, and 30% sucrose) and kept frozen at $-80°C$. The brains were sectioned in cryostat starting at mid-sagittal plane laterally at 20 μm thickness, with every other section (1st, 3rd, 5th…) used for immunohistochemical study.

Immunohistochemistry

Frozen sections were thawed, and immersed in PBS. Antigen retrieval was done in 10 mM citrate buffer (pH = 6.0) for 25 min, with subsequent peroxidase quenching in 3% H_2O_2/methanol. All the sections were blocked in 2% milk overnight and probed either with anti-NG2 rabbit polyclonal antibody, 1:500 (Millipore) or anti-GFAP mouse monoclonal antibody 1:400 (Sigma) diluted in 2% milk for 16 h at 4°C. Detection of bound antibody was done using appropriate HRP-conjugated secondary antibodies in VECTA-STAIN kit (Vector Labs) according to manufacturer's protocol. Reaction product was enhanced with DAB (1:25 dilution) for 6–10 min, with subsequent dehydration in ethanol. The slides were mounted with Gel Mount, coverslipped and dried. Images were acquired on Nikon bright-field microscope equipped with digital camera. To quantitate the number of oligodendrocyte progenitors and astrocytes in each treatment group, random sections (four per animal, total of $N = 5$ animals per treatment group) of genu corpus callosum stained for NG2 and GFAP markers, which were counted by two blinded investigators at 40× magnification. Only the cells where process branching and the nucleus was clearly visible were counted. This approach eliminated endothelial cells that were stained by NG2 antibody. The cell counts were expressed as number of cells per 40× field and represent pooled data from two independent investigators. The data were evaluated for statistical significance using unpaired t-test.

Primary Cultures

Primary cultures were prepared from newborn rat pups of CRL SD rats according to standard protocol of McCarthy and de Vellis (1980). Briefly, newborn rat pups were decapitated and heads immersed in 70% ethanol, following by extensive washing with Hank's balanced salt solution. The brain was extracted and meninges carefully removed. The cerebral tissue was diced and trypsinized for 30 min. Following digestion with DNAse I, the tissue homogenate was passed through 150 and 75 μm Nitex screens. Filtered cells were resuspended in plating medium (DMEM/10% FBS) and cultured for 8 days. To purify different types of glia, mixed glial cultures obtained in this way were subjected to a serial shaking purification protocol (McCarthy and de Vellis 1980). First, the microglia was removed by shaking for 1 h at 265 rpms. Subsequently, oligodendrocyte progenitor cells were removed by shaking for 18 h at 265 rpms. The remaining astrocytes were allowed to recover for one day, and then collected by trypsinization, counted and plated for experiments in poly-D-lysine coated 24-well plates. The oligodendrocyte progenitor fraction was subsequently further purified by differential adhesion through incubation in Petri dish for 30 min to remove more adherent astrocytic and microglial contamination. This procedure routinely yielded >90% pure population of OPCs (verified by A2B5 staining, not shown). These cells were then re-plated in poly-D-lysine coated 24-well plates or 4-well chamber slides in N2S media (composition described by Bottenstein 1986; Zhang et al. 2005) and used for experiments.

Immunostaining of OPCs for H-ferritin

Primary rat OPCs plated in chamber slides were washed in PBS fixed for 5 min in freshly prepared ice-cold 4% paraformaldehyde for 5 min. After two washes in PBS, cells were air dried and frozen at $-80°C$. The day of the experiment, cells were thawed and permeabilized in 0.1% Triton X100 for 5 min. After three washes in PBS, cells were blocked in 10% Normal Goat Serum (NGS) for 16 h, with exposure to primary antibodies diluted in 1.5% NGS for 16 h. The primary antibodies used were anti-H-ferritin rabbit polyclonal 1:100 (Cheepsunthorn et al. 1998) and anti-A2B5 mouse IgM 1:100 (R&D Systems). Nuclei were stained with DAPI at 1:750 dilution (Invitrogen). Staining was visualized with anti-rabbit-AF488 and anti-mouse IgM-AF555 antibodies (Molecular Probes) at 1:150 dilution for 1.5 h. Images were acquired at Leica confocal microscope.

Cytotoxicity Assays and Apoptosis Analysis

Primary cells (oligodendrocytes or astrocytes) were treated with Na-metavanadate or Na-metavanadate plus DFO at different concentrations. Untreated cells (with vehicle) served as control. In all experiments, cells were exposed to these experimental conditions for 48 h, unless indicated otherwise. The cell viability was determined using MTT

assay according to manufacturer's protocol, and absorbance measured on plate reader at 595 nm. All absorbance values were normalized to control to obtain percent survival. Alternatively, for apoptosis detection cells were washed with PBS (pH = 7.4) for 5 min and then exposed to Annexin V-AlexaFluor488 (Molecular Probes) in Annexin binding buffer at 1:25 dilution for 40 min. Cells were washed in binding buffer and visualized under Nikon fluorescence microscope. Representative images of Annexin binding to treated OPCs in random fields were reproduced, and Annexin V-labeled cells counted in five random fields for each experimental condition in triplicates by an experimenter blinded to the experimental condition. The counts in different experimental groups were averaged and evaluated for statistical significance using one-way ANOVA.

Intracellular ROS Measurements

Primary rat OPCs were plated at a concentration of 0.5 million cells per well in 6-well plates. The cells were treated with 100 μM Na-metavanadate in N2S media for 6 h. Subsequently, cells were washed in warm Hank's buffer and incubated with 10 μM 2′-7′-dichlorofluorescein (DCFH-DA; Calbiochem) diacetate dye for 1 h as previously described (Mawatari et al. 1996). After incubation, the cells were collected mechanically, resuspended in PBS buffer and aliquoted in 96-well plates. Fluorescence was measured on Gemini SpectraMAX plate reader with 495 nm excitation and 515 nm emission spectra. The obtained fluorescence values were averaged and evaluated for statistical significance using unpaired t-test.

Ferritins

Purified horse spleen ferritin (SF) and horse spleen apoferritin (Apo-SF) were obtained from Calbiochem. Recombinant human H-ferritin cDNA tagged with polyhistidine was subcloned into peT plasmid, amplified, verified by sequencing. The plasmid was transformed into competent BL21 *E. coli* and protein overexpression induced with IPTG (isopropyl-β-D-thio-galactoside) when the OD value of bacterial culture reached 0.7. The recombinant H-ferritin was purified over Nickel column (Pierce) according to the manufacturer's protocol as described previously (Todorich et al. 2008). The identity and purity were verified by Western blot (anti-human H-ferritin HS-59 monoconal antibody, generous gift from Dr. Paolo Arosio) and purity by Comassie staining of SDS PAGE gel with 10 μg of protein loaded per well, respectively. We verified the presence of ferroxidase activity of this recombinant protein by measuring rate of oxidation of ferrous into ferric iron at 310 nm absorbance (Fig. 6b). We

incubated 100 μl of 0.4 μg/μl rH-ferritin in PBS solution (pH = 7.4) with an aliquot of ferrous sulfate; the same experiment with PBS alone (no ferritin) served as a control of auto-oxidation rate of ferrous sulfate in PBS buffer. We monitored time-dependent formation of ferric iron in solution by measuring absorbance at 310 nm. The results in Fig. 6b show that the presence of recombinant H-ferritin increase speed and amount of ferric iron formation compared to baseline auto-oxidation of the same in PBS buffer alone as detected by time-dependent increase in absorbance at 310 nm. To evaluate interaction between ferritin, iron, and vanadium exposure in OPCs, we exposed primary rat OPCs to 100 μM vanadium in the presence of increasing concentrations of TMH-Fe or recombinant H-ferritin for 48 h. Untreated cells and OPCs treated with TMH-Fe or H-ferritin alone served as baseline controls. The cell viability was determined by MTT assay, with total absorbances determined at 595 nm, and expressed as percentage of untreated control to obtain percent survival (Fig. 6c, d).

Ferritin-Iron Release and DNA Relaxation Assay

Supercoiled DNA relaxation assay was used to determine mechanism of vanadium-induced iron release from ferritin as described previously (Surguladze et al. 2004). This assay uses supercoiled DNA that runs as a low-MW ladder on agarose gel whose nicking in response to ferritin is highly dependent on release of free iron that catalyzes production of free radicals. As a result, single strand breaks (resulting in relaxed form of the plasmid, high MW band) and/or double strand breaks (resulting in linear form of the plasmid, intermediate MW band) were produced proportionally to the amount of redox active iron released from ferritin (Surguladze et al. 2004). The pUC19 supercoiled DNA plasmid (New England Biolabs) was incubated with vanadate alone or various recombinant ferritins either alone or in the presence of vanadate. The reaction mixtures (20–30 μl) contained DNA (0.5 or 1 μg), dissolved in 10 mM HEPES (pH 7.5), 50 mM NaCl, 2.5 mM MgCl$_2$, 2.5 mM DTT. Reactions with ferritins, DNA and vanadium were incubated for increasing time duration and quenched by addition of 10 μL of 50% glycerol, 50 mM EDTA, 50 mM EGTA, and 0.1% bromophenol blue. The samples are separated using 1.5% agarose gel run in 40 mM Tris–acetate, 1 mM EDTA (TAE), pH 8.0. The DNA bands were visualized using SYBR green staining (Invitrogen) according to manufacturer's protocol.

Results

To investigate the in vivo effects of vanadium exposure on myelin producing cells in CNS, we exposed newborn rats

for the first two weeks after birth to daily injections of 3 mg/kg sodium metavanadate. Littermate rats of same sex receiving same volume of PBS served as controls. The vanadium-treated rat pups had a comparable, although slightly decreased (statistically significant at several time points), rate of weight gain in the first two weeks of development (Fig. 1a). The pups receiving vanadium injections had a substantial impairment in motor function at P15 as demonstrated by rotarod testing (Fig. 1b). Upon histological examination of the brains of the P15 rat pups, we observed a 2.5-fold decrease in the number of NG2-positive oligodendrocyte progenitors in the genu of corpus callosum of vanadium-treated rats compared to controls (Fig. 2a, b, e). Conversely, the number of astrocytes in the same region of corpus callosum was increased in the vanadium-treated group (Fig. 2c, d, f), and astrocytes of the vanadium-treated group had more extensive branching suggestive of activation (Fig. 2c, d).

The in vivo data suggested that vanadium was cytotoxic to oligodendrocytes, but stimulated astrogliosis. To investigate whether this observed effect in vivo is due to the differences in the relative sensitivity of glial cells to cytotoxic effect of vanadium compounds, we generated primary rat cultures enriched in oligodendrocyte progenitor cells, mature oligodendrocytes, and astrocytes. The enriched cultures of different glia (OPCs, mature oligodendrocytes, and astrocytes) were exposed to increasing concentrations of Na-metavanadate for 48 h. The cell viability was determined using MTT assay, and absorbance normalized to control (untreated) to obtain percent survival. While vanadium was cytotoxic in dose-dependent manner to all three cell types studied, the primary OPCs were much more sensitive to vanadate exposure than

astrocytes or mature oligodendrocytes. By comparing the same concentration of metavanadate treatment across different cells types, we found the primary OPCs had a LD50 of approximately 75 μM, while the LD50 was approximately 200 μM for primary astrocytes and mature oligodendrocytes (Fig. 3a–c).

To begin to examine the mechanism of cell stress and cytotoxicity induced by vanadium exposure in OPCs, we measured ROS generation in OPCs using dichlorofluorescein dye (DCF). Vanadium exposure in OPCs resulted in nearly 3-fold increase in DCF flourescence compared to baseline in control (untreated cells) (Fig. 4a). We also determined that exposure to Na-metavanadate resulted in inversion of phosphatidyl serine at the membrane, as detected by AnnexinV labeling, suggestive of apoptosis (Fig. 4b). At 12 h post-treatment, 100 μM Na-metavanadate produced 10-fold increase in number of annexinV-positive cells compared to the untreated control. Collectively, these data suggest that induction of oxidative stress and apoptosis underlie cytotoxic mechanism of vanadium exposure in oligodendrocyte progenitors.

To investigate a possible relationship between iron and vanadium toxicity in oligodendrocyte progenitors, we exposed primary rat OPCs to 100 μM Na-metavanadate with or without concurrent treatment with increasing concentrations of iron chelator desferroxamine (DFO) for 48 h, and then analyzed morphology and cell viability using bright-field microscopy and a MTT assay, respectively. Vanadium-treated oligodendrocyte progenitor cells had retracted processes and membrane fragmentation was clearly visible at 48 h post-treatment, whereas, the control (untreated cells) have extended and ramified processes (Fig. 5a, b). Furthermore, the cell morphology including
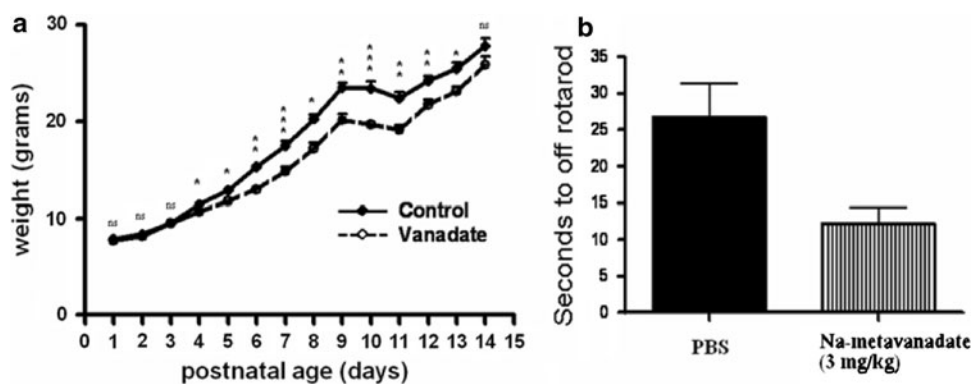
Fig. 1 Vanadium exposure during early post-natal period leads to impaired motor functioning. Newborn rat pups were injected with 3 mg/kg body weight of Na-metavanadate solution IP once per day for 14 days (N = 5). Injection of equal volume of PBS to littermate siblings served as control (N = 5). Each day, weights of the pups were measured and plotted as means with standard deviation (a). The mean weights at each day were evaluated for statistical significance using paired t-test at each time point (ns, not significant; * P < 0.05;

** P < 0.01; *** P < 0.0001). At P15, vanadium-treated and control rats were subjected to rotarod testing of motor function. Each rat was evaluated in three independent trials with rest periods in between. The time from start of rotarod to the moment that the rat fell of the rotarod was recorded by two blinded investigators (b). The values were averaged and evaluated for significance using one-sided t-test (** P < 0.01)

Fig. 2 In vivo, vanadium exposure during early post-natal period results in a decreased number of NG-2 positive oligodendrocyte progenitors and increased GFAP-positive astrocytes in genu corpus callosum of P15 rat. Beginning at birth, rat pups were injected with vanadium (3 mg/kg IP once daily) or PBS (IP once daily) until P15. The rats were killed and sagittal sections of the brain stained for NG-2 and GFAP markers. For this panel, representative images taken from random fields showing NG2-positive OPCs (**a**, **b**), and GFAP-positive astrocytes (**c**, **d**) in genu corpus callosum of metavanadate treated and control (PBS) rats. The number of NG2-positive and GFAP-positive cells were counted by two blinded investigators and averages of $N = 5$ per group counts are shown per high-powered field (HPF, $40\times$) in (**e**) and (**f**), respectively. The differences between groups were evaluated for significance using unpaired t-test (* $P < 0.05$; ** $P < 0.01$)
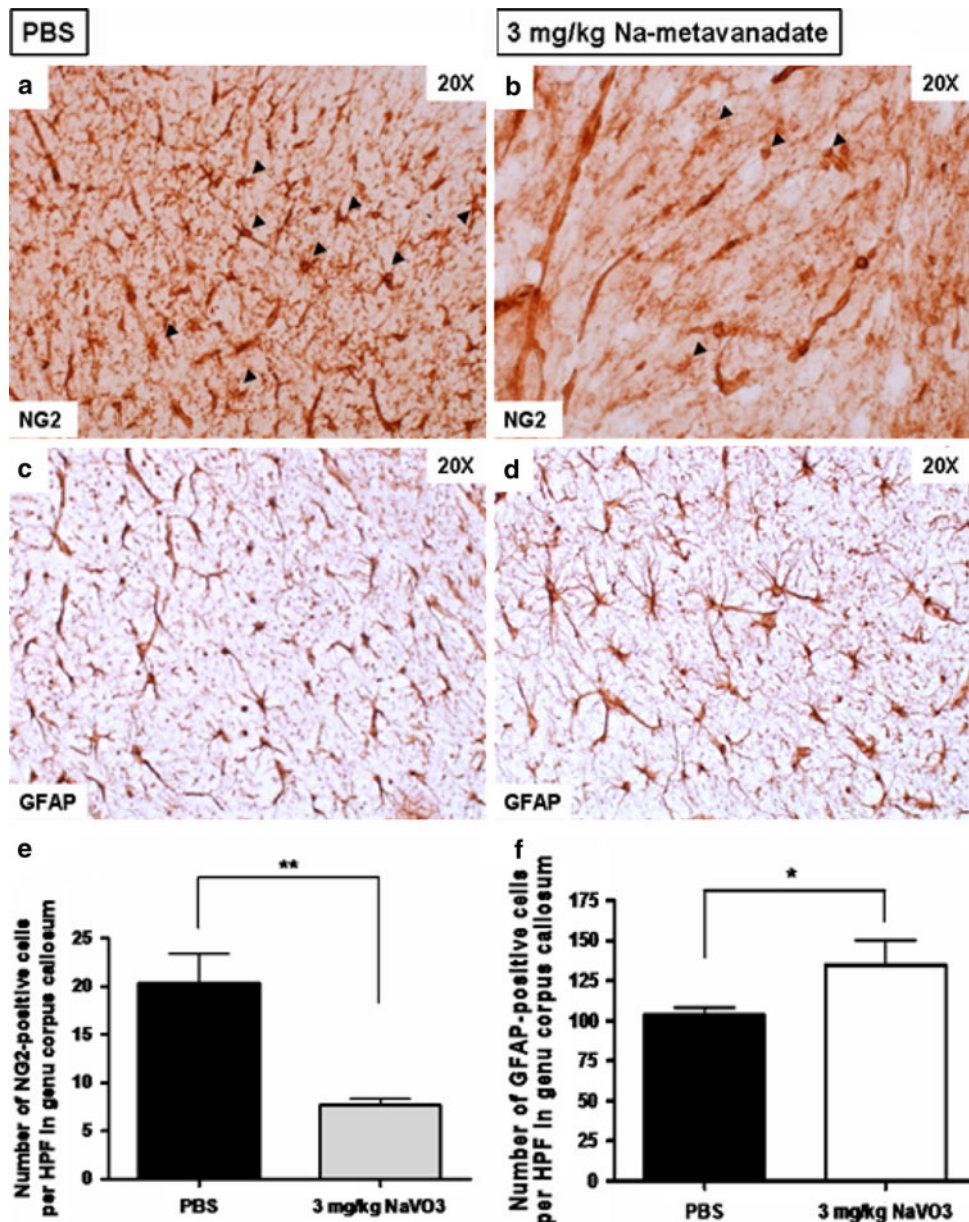

branching was preserved when 100 μM DFO was co-incubated with the vanadium (Fig. 5c). Cell viability was determined by MTT assay. In Fig. 5d, we show that 100 μM vanadium kills 70% of primary OPCs, an effect that was partially reversed by different concentration of iron chelator DFO. A similar effect is seen with vanadium-induced apoptosis in OPCs; vanadium treatment significantly increases annexinV labeling of OPCs while 100 μM DFO co-treated OPCs had annexinV staining similar to baseline levels (Fig. 5e). These data suggested that the limiting iron availability to OPCs at the time of vanadium exposure provided partial protection from vanadium-induced cytotoxicity.

As mentioned, iron acquisition by oligodendrocytes seems to be a key step in the oligodendrocytes maturation and the ability of an iron chelator to limit vanadium-related damage to the OPCs suggest a potential interaction. Iron acquisition and management in developing oligodendrocytes appears to involve expression of cytosolic ferritin and delivery of iron via endocytosis of extracellular H-ferritin (Cheepsunthorn et al. 1998; Hulet et al. 2000; Todorich et al. 2008). Primary rat OPCs were treated either with 100 μM Na-metavanadate alone or in the presence of increasing concentration of recombinant human H-ferritin for 48 h, and the cell viability at the time measured using MTT assay. The results summarized in Fig. 6c show that
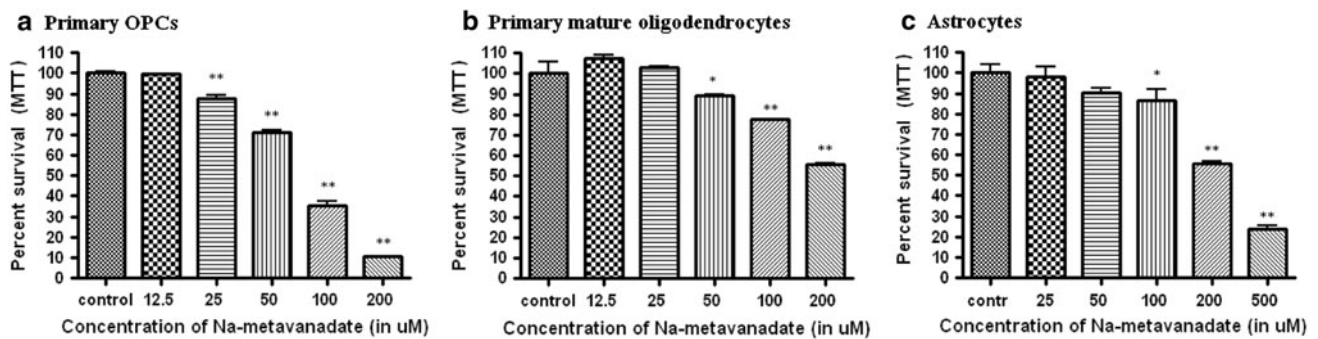
Fig. 3 In vitro, primary oligodendrocyte progenitors (OPCs) are more vulnerable to cytotoxic effects of vanadium than mature oligodendrocytes or astrocytes. Primary astrocytes, OPCs and mature oligodendrocytes were exposed to increased concentrations of Na-metavanadate for 48 h. MTT reagent was added for last 4 h of treatment, cells solubilized and absorbances measured at 595 nm. All absorbance values were normalized to controls to obtain % survival. The means were evaluated for significance using one-way ANOVA with Dunnett's post-test comparison to the control group. Only the indicated groups are statistically significant (* $P < 0.05$; ** $P < 0.01$). The data are means of at least three different independent experiments
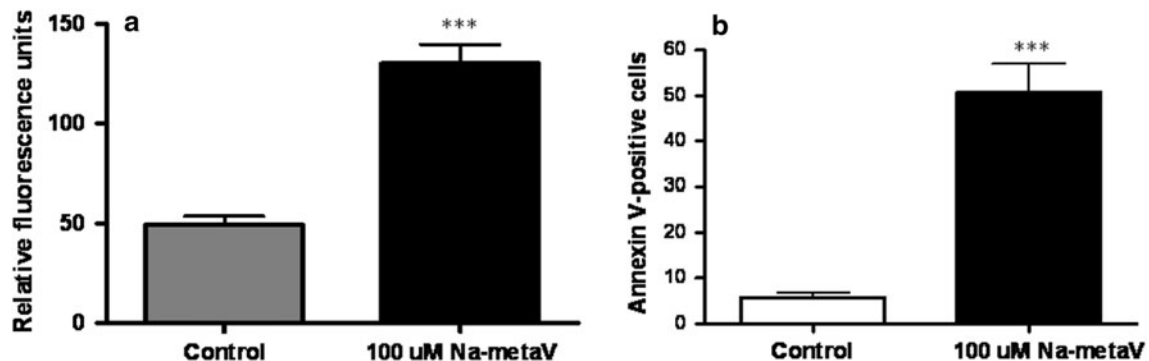

Fig. 4 Vanadium exposure increases ROS generation and apoptosis of primary oligodendrocyte progenitors in culture. Primary rat OPCs were exposed to 100 μM Na-metavanadate or vehicle (PBS) as control for 6 h (ROS measurement) and 12 h (apoptosis determination). Intracellular ROS generation was detected by incubating cells with dichlorofluorescein dye (DCF) for 1 h at 37°C, and measuring relative fluorescence in equal number of cells in vanadium-treated and control groups. Panel **a** reveals 2.5-fold increases in measurable ROS production in response to vanadium exposure 6 h post treatment. The average fluorescence of three independent experiments (subtracted for background) was plotted and analyzed for significance using unpaired t-test (*** $P < 0.001$). (**b**) At 12 h time point, vanadium-treated and control cells were exposed to alexa-fluor 488 conjugated annexinV dye, and bound fluorescence detected on Nikon fluorescence microscope at 10× magnification. Random images captured were counted for annexinV-positive cells in four quadrants by an investigator blinded to the experimental condition. The averages for each group were analyzed for significance using unpaired t-test (*** $P < 0.001$)

increasing concentrations of recombinant H-ferritin exacerbated cytotoxic effect of Na-metavanadate on primary rat OPCs as measured by the MTT assay. The same concentrations of recombinant H-ferritin without vanadium had no significant effect on viability of OPCs. When primary OPCs were exposed to the increasing concentrations of TMH-ferrocene (a lipophilic compound that can deliver iron into cells independent of iron-import proteins), in the presence of Na-metavandate, a dose-dependent relationship was observed (Fig. 6d). There was no effect on OPC cell viability when the highest concentration of TMH-ferrocene was used alone. These data indicate that increasing iron availability to OPCs exacerbates cytotoxic effects of vanadium, and that vanadium interaction with H-ferritin may be an important determinant of oligodendrocyte survival.

Because of their high iron content and high iron utilization, mature oligodendrocytes also express high levels of endogenous H-ferritin (Connor et al. 1994; Connor and Menzies 1996; Connor et al. 1990). To show that this is also true in oligodendrocyte progenitors we immunostained OPCs for H-ferritin. In Fig. 7 we demonstrate that H-ferritin immunoreactivity within A2B5-positive oligodendrocyte progenitor cells in culture is primarily localized in perinuclear region of the cell body. There was minimal staining of the cell processes and no staining in cells where primary antibody to H-ferritin was omitted (data not shown). These results are important to our interpretation of the vanadium toxicity results where we propose that vanadium may interfere with iron homeostasis by interacting with endogenous (cytosolic) ferritins in addition to
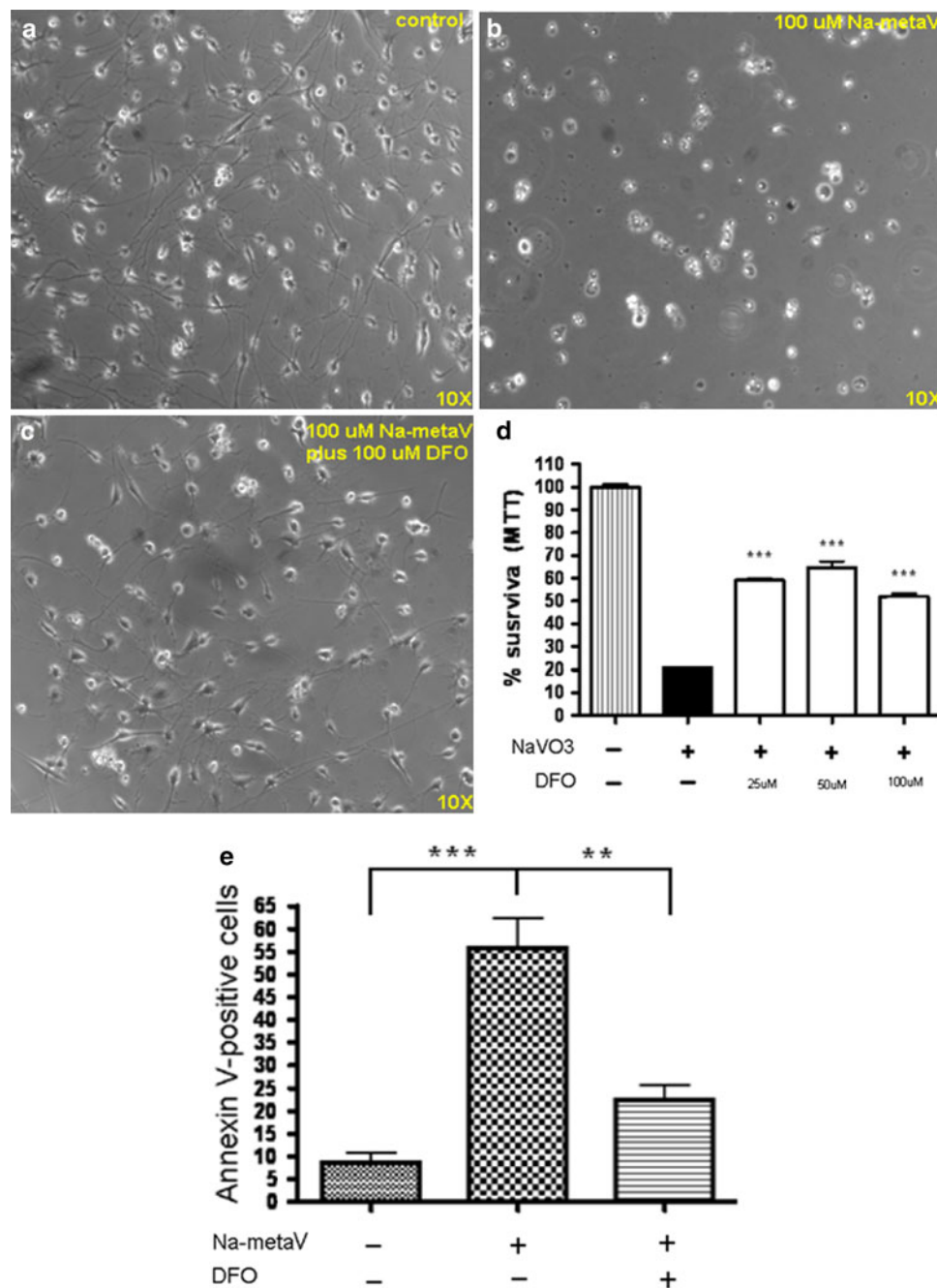
Fig. 5 Iron chelator desferroxamine (DFO) protects oligodendrocyte progenitors from vanadium-induced cytotoxicity and apoptosis. Primary rat oligodendrocyte progenitors were treated with 100 μM Na-metavanadate alone or with increasing concentrations of DFO. The untreated cells served as control. Representative bright-field images of OPCs, control (untreated), 100 μM vanadium treated without and with 100 μM DFO at 48 h post-treatment (**a**, **b**, **c**). Images demonstrate loss of cell viability, process collapse, and detachment from the surface of the dish in vanadium-treated cells, which is completely prevented by co-administration of 100 μM DFO. The findings were confirmed by quantitation using MTT assay for cell viability (**d**). These data show that increasing concentrations of DFO reverse 48 h cytotoxicity of 100 μM Na-metavanadate on primary rat OPCs. The absorbance obtained at 595 nm was normalized to the control group to obtain the percentage survival for each experimental group. The statistical differences were determined using one-way ANOVA with Dunnett's post-test comparisons. All data in the figure are representative of at least three independent experiments. (**e**) At 12 h post-treatment, 100 μM DFO reduces the extent of apoptotic phosphatidyl serine inversion of Na-metavanadate-treated OPCs as detected by Annexin-AF488 labeling. Random images obtained on Nikon fluorescent microscope were counted by an investigator blinded to the experimental condition. The means were analyzed for statistical significance using one-way ANOVA with Tukey's post-test comparisons between multiple groups. The indicated group comparisons were significant (** $P < 0.01$, *** $P < 0.001$). The data are representative of three independent experiments
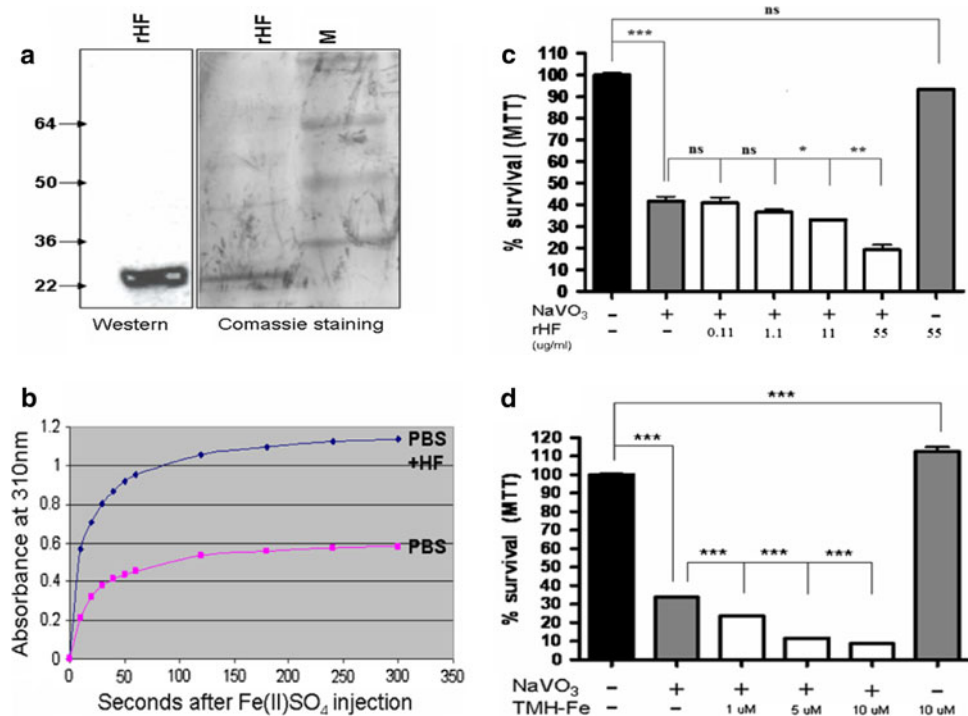
Fig. 6 Adding recombinant H-ferritin or lipophilic iron delivery compound, TMH-ferrocene increase vulnerability of primary rat OPCs to vanadium cytotoxicity. (**a**) Recombinant His-tagged human ferritin heavy chain (rHF) was prepared in BL21 *E. coli* and purified over Nickel column, with identity and purity verified by Western blot and Comassie staining of denaturing gel. Both show characteristic bands at 22 kDa consistent with ferritin monomers. M is the lane denoting molecular weight markers. (**b**) The enzymatic activity of the ferroxidase of recombinant H-ferritin was verified by its ability to oxidize ferrous iron in solution. The solution of 0.4 µg/µl rH-ferritin in PBS (pH = 7.4) was incubated with a single injection of ferrous sulfate, and formation of ferric iron was monitored by measuring absorbance at 310 nm (detects amber color associated with ferric iron formation). Presence of recombinant H-ferritin in solution significantly increases rate and the amount of ferritic iron formed compared to auto-oxidation of ferrous iron in PBS alone, suggesting that recombinant H-ferritin possesses significant ferroxidase activity. (**c, d**) Primary rat OPCs were exposed to 100 µM Na-metavanadate either alone or in the presence of increasing concentrations of recombinant H-ferritin (**c**) or TMH-ferrocene (**d**). The dose-dependent exacerbation of the cytotoxic effect of vanadium was quantified by MTT assay. All absorbance values were normalized to control and expressed as percent survival. Statistical significance was determined by one-way ANOVA with Bonnferonni's post-test comparisons between multiple groups. Comparisons between control (untreated) and vanadium or H-ferritin/TMH-Fe only groups are indicated, as well as comparisons between vanadium only and vanadium with rHF/TMH-Fe groups (* $P < 0.05$, ** $P < 0.01$, *** $P < 0.001$). The data are representative of at least two independent experiments (**d**)

iron assimilation through extracellular H-ferritin in oligodendrocyte progenitors.

To test a hypothesis that exacerbating effect of ferritin on vanadium-mediated cytotoxicity is due to release of redox active iron from ferritin, we used DNA relaxation/nicking assay previously characterized in our laboratory (Surguladze et al. 2004). Incubating supercoiled DNA plasmid (puc19) with increasing concentrations of vanadium (25–200 µM) alone failed to produce either relaxed or linearized forms of DNA (Fig. 8a–d). Incubating puc19 plasmid with horse spleen ferritin (iron-rich) alone resulted in a time-dependent conversion to the relaxed form (single strand nicking), but no visible linearization (double strand nicking Fig. 8e1–e7). However, this effect was greatly augmented when iron-rich spleen ferritin was co-incubated with 200 µM Na-metavanadate, increasing amounts of relaxed DNA (arrow 3) and linear DNA from double nicks (arrow 2) (red box). No DNA nicking was produced in apo-spleen ferritin alone or in combination with 200 µM Na-metavanadate (Fig. 8g1–7, h1–7). These results suggest that the synergistic relationship between vanadium and ferritin on vanadate-mediated cytotoxicity is through increased redox active iron release.

Discussion

In this study, we investigated cellular and molecular mechanisms of hypomyelination due to developmental vanadium exposure. We demonstrate that oligodendrocyte progenitors are vulnerable to vanadium exposure both in vivo and in vitro, suggesting a potential direct cellular

Fig. 7 Oligodendrocyte progenitors in culture express endogenous cytosolic H-ferritin. Rat primary oligodendrocyte progenitors were stained with antibodies for H-ferritin (**a**) and A2B5 marker (**b**), and were visualized with Alexa-flour 488 and 555 secondary antibodies, respectively. DAPI was used as a nuclear stain (**c**) and overlay projection is shown in (**d**). Representative confocal images of two independent experiments demonstrate primarily perinuclear localization of H-ferritin expression (*yellow arrows*) in A2B5-positive oligodendrocyte progenitors with minimal staining of oligodendrocyte processes
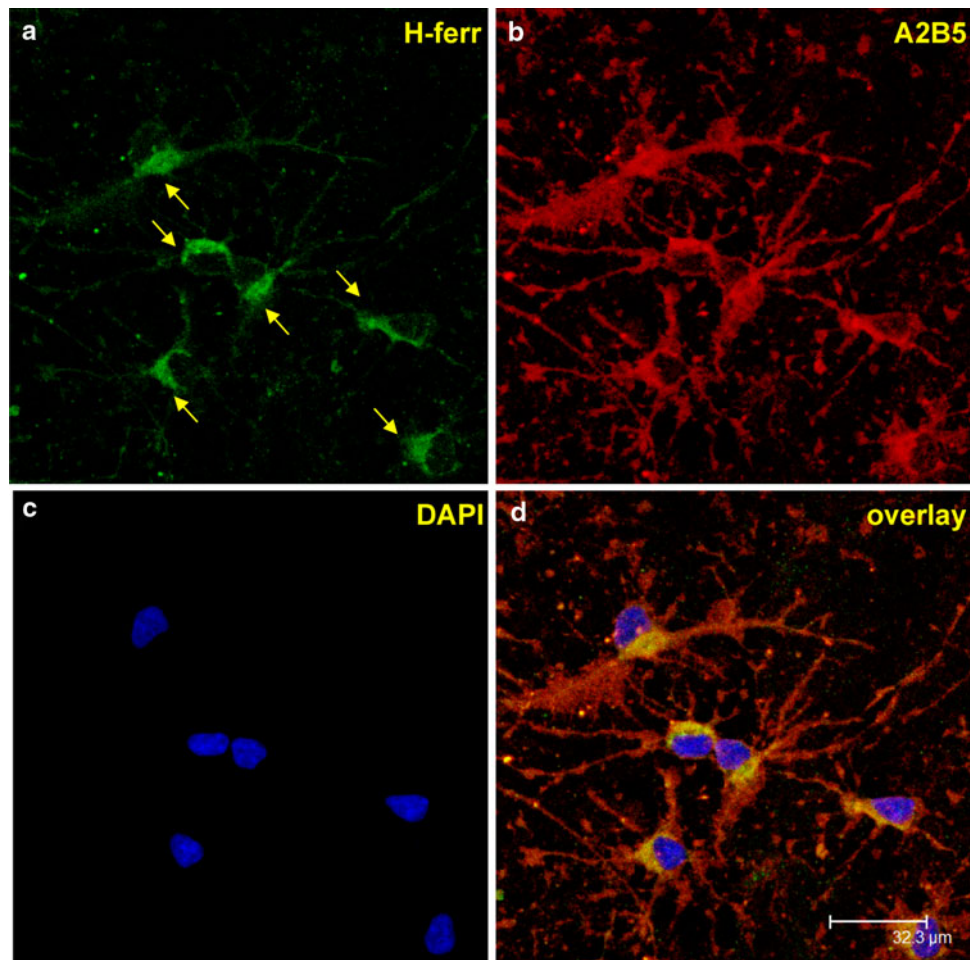
mechanism for vanadium-induced hypomyelination. Furthermore, our data suggest that the mechanism underlying vanadium destruction of OPCs involves increased oxidative stress and apoptosis of these cells. Because iron is a key component of oligodendrocyte maturation and because vanadium binds to transferrin and ferritin proteins (EVM 2002; Monteiro et al. 1991; Sabbioni and Marafante 1981; Sabbioni et al. 1980), we manipulated the iron availability to oligodendrocytes in the presence of vanadium. The apoptotic indices and cytotoxicity of vanadium on OPCs were significantly increased with co-exposure to the lipophilic iron compound TMH-ferrocene and decreased by exposure to the iron chelator DFO, which suggested the role of free iron in cytotoxic mechanisms of vanadium even though a direct chelating effect of DFO on vanadium could not be ruled out. The positive effect of the iron chelator suggested that ferritin, an iron sequestering protein, should have limited iron related damage. Furthermore, ferritin has been consistently associated with cytoprotection (Harrison and Arosio 1996). Unexpectedly, our data demonstrated that the presence of ferritin exacerbated the vanadium-induced damage. Thus, we evaluated the possibility that vanadium promoted the release of iron from ferritin using a supercoiled DNA relaxation assay. We demonstrate that vanadium causes release of iron from ferritin, and that co-exposure of OPCs with ferritin or iron increases vulnerability of these cells to cytotoxic effects of vanadium. Because oligodendrocyte progenitors import iron through ferritin in early development (Todorich et al. 2008, 2009), and express significant levels of endogenous ferritin (Cheepsunthorn et al. 1998), we propose that this dependence on ferritin is what makes OPCs relatively vulnerable to pro-apoptotic effects of vanadium exposure. How vanadium promotes iron release and/or inhibits iron assimilation into ferritin is beyond the scope of this study, but one possible explanation is that the larger ionic radius of vanadium (relative to iron) results in structural changes and instability of the ferritin 24-mer as ferritin attempts to sequester vanadium from solution. This effect would impair ferritin function in iron uptake and promote iron release and/or target ferritin for degradation with subsequent iron release. The other possibility is that vanadium releases iron through a reductive mechanism by direct interaction with the ferric hydrite crystals at the ferritin core.

In vivo experiments on vanadium neurotoxicity have suggested that hypomyelination is one of the main
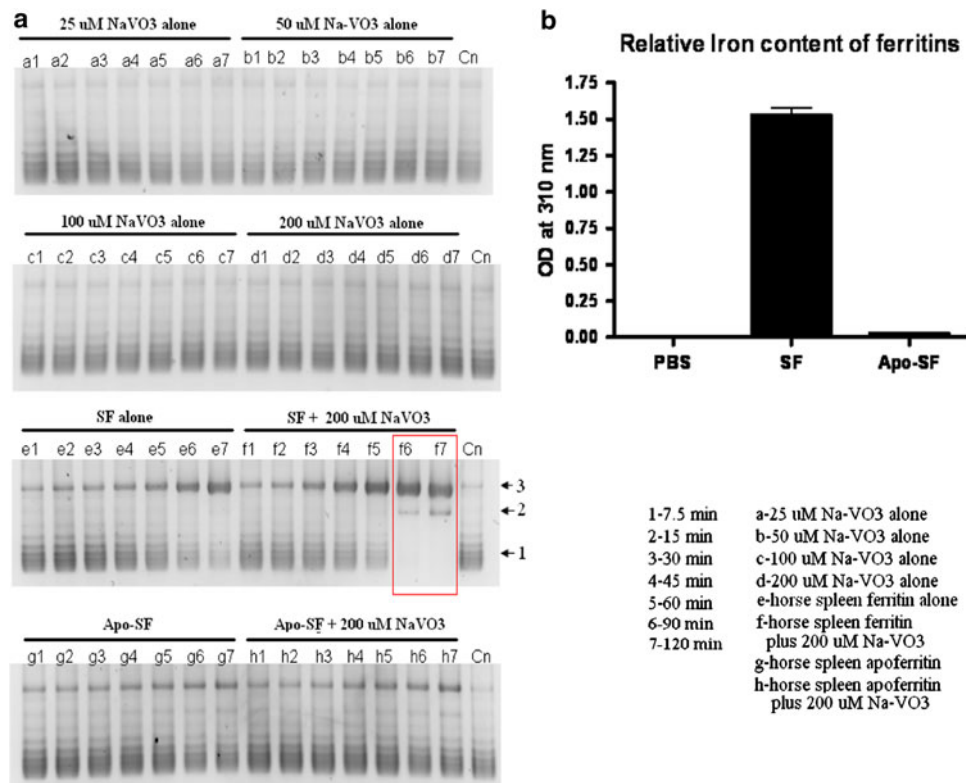
Fig. 8 Vanadium interacts with iron-rich ferritins to induce single and double strand breaks in supercoiled DNA relaxation assay. (**a**) Increasing concentration of vanadium (a 25 μM; b 50 μM; c 100 μM; and d 200 μM) were co-incubated with puc19 plasmid DNA for 7.5–120 min. Lane with puc19 without vanadium (Cn) served as a control. Vanadium alone did not have any effect on DNA (lanes a, b, c, and d, 1–7). Incubating iron-rich horse spleen ferritin (e) alone with DNA (*arrow* 1) caused time-dependent DNA relaxation/ss nicking (*arrow* 3), but not linearization/ds nicking (*arrow* 2). The effect was significantly augmented in same experiment with addition of 200 μM Na-metavanadate, producing both single (*arrow* 3) and double stranded nicks (*arrow* 2) in puc19 DNA (*red box*, f6, f7). None of these effects were observed if iron-poor horse spleen apo-ferritin is used, even in the presence of 200 μM Na-metavanadate. (**b**) Shows absorbance of horse spleen ferritin (SF) and horse spleen apo-ferritin (apo-SF) at 310 nm as a surrogate marker of iron content. PBS alone was used as a baseline measurement (blank)

pathological outcomes in the brain of toxic vanadium exposure (Garcia et al. 2004). We hypothesized that hypomyelinating effects of vanadium exposure are due to destruction of developing oligodendrocytes. To test our hypothesis in vivo, we injected newborn rat pups with 3 mg/kg of sodium metavanadate IP once daily in for the first two postnatal weeks of development. These mice had significant motor performance deficits when compared to vehicle-treated controls. Accompanying the motor deficits was a 2.5-fold decrease in number of NG2 positive oligodendrocyte progenitors in genu corpus callosum. Our in vivo observations suggested that oligodendrocyte progenitors, but not astrocytes are more susceptible to vanadium exposure in the early postnatal period; an observation and interpretation supported by the cell culture models. These data indicate that the loss of OPCs may contribute to the hypomyelination following developmental vanadium exposure. The higher susceptibility of the OPCs to vanadium than either mature oligodendrocytes or astrocytes may be explained by their relatively low expression of antioxidant defenses, such as glutathione

(Hemdan and Almazan 2007; Husain and Juurlink 1995; Juurlink et al. 1998; Thorburne and Juurlink 1996). In support of the oxidative stress mechanism underlying vanadium exposure to OPCs, we observed elevated markers of apoptosis and oxidative stress in these cells. Vanadium can produce ROS either directly through Fenton-like reaction (Evangelou 2002) or as we report herein, by promoting unregulated release of highly redox active iron from ferritin stores (Fig. 9).

In toto, the studies described herein report in vivo and in vitro evidence of cellular and molecular mechanisms that may contribute to demyelination caused by vanadium exposure in the early post-natal period. Our findings suggest that vanadium targets oligodendrocyte progenitors in the early post-natal period by taking advantage of their relatively high iron requirements and their dependence on ferritin for iron storage and delivery as well as their diminished antioxidant capacity. The relationship between iron and vanadium warrants further comment on the environmental exposure to vanadium in cultures where iron deficiency is prevalent. Iron deficiency itself carries a
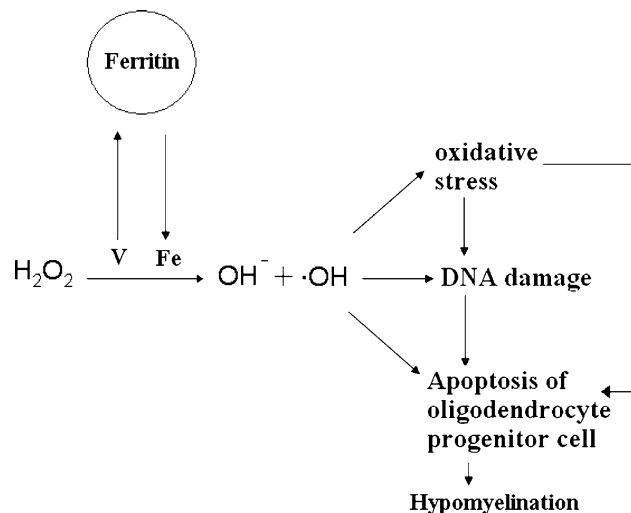
Fig. 9 Our current understanding of mechanisms of vanadium-mediated oligodendrocyte cell injury. As a transition metal, vanadium participates in redox reactions, contributing to the generation of ROS (toxic hydroxyl radical) through Fenton-like mechanism. In addition, our findings suggest that vanadium can promote release of redox active iron from the stores in ferritin, which further exacerbates ROS generation, cellular toxicity leading to apoptosis, and destruction of oligodendrocyte progenitors

neurological burden of hypomyelination. Where iron deficiency is a nutritional problem and vanadium exposure an environmental concern, the dual effect could be clinically devastating. With iron deficiency, transferrin is elevated and thus could transport more vanadium if this metal were more abundant. In fact, in the rat model of iron deficiency, increased levels of various metals including vanadium in the brain have been documented (Garcia et al. 2007). If the decreased iron and associated hypomyelination would be exacerbated by vanadium toxicity is an important health issue that should receive additional investigation based on the findings of this report.

References

Bottenstein JE (1986) Growth requirements in vitro of oligodendrocyte cell lines and neonatal rat brain oligodendrocytes. Proc Natl Acad Sci USA 83(6):1955–1959

Cheepsunthorn P, Palmer C, Connor JR (1998) Cellular distribution of ferritin subunits in postnatal rat brain. J Comp Neurol 400(1):73–86

Connor JR, Menzies SL (1996) Relationship of iron to oligodendrocytes and myelination. Glia 17(2):83–93

Connor JR, Menzies SL, St Martin SM, Mufson EJ (1990) Cellular distribution of transferrin, ferritin, and iron in normal and aged human brains. J Neurosci Res 27(4):595–611

Connor JR, Boeshore KL, Benkovic SA, Menzies SL (1994) Isoforms of ferritin have a specific cellular distribution in the brain. J Neurosci Res 37(4):461–465

Degani H, Gochin M, Karlish SJ, Shechter Y (1981) Electron paramagnetic resonance studies and insulin-like effects of vanadium in rat adipocytes. Biochemistry 20(20):5795–5799

Evangelou AM (2002) Vanadium in cancer treatment. Crit Rev Oncol Hematol 42(3):249–265

EVM (2002) Expert group on vitamins and minerals. Review of vanadium. EVM/00/04:1-16

Garcia GB, Quiroga AD, Sturtz N, Martinez AI, Biancardi ME (2004) Morphological alterations of central nervous system (CNS) myelin in vanadium (V)-exposed adult rats. Drug Chem Toxicol 27(3):281–293

Garcia SJ, Gellein K, Syversen T, Aschner M (2007) Iron deficient and manganese supplemented diets alter metals and transporters in the developing rat brain. Toxicol Sci 95(1):205–214

Haider SS, Abdel-Gayoum AA, el-Fakhri M, Ghwarsha KM (1998) Effect of selenium on vanadium toxicity in different regions of rat brain. Hum Exp Toxicol 17(1):23–28

Harrison PM, Arosio P (1996) The ferritins: molecular properties, iron storage function and cellular regulation. Biochim Biophys Acta 1275:161–203

Heinz A, Rubinson KA, Grantham JJ (1982) The transport and accumulation of oxyvanadium compounds in human erythrocytes in vitro. J Lab Clin Med 100(4):593–612

Hemdan S, Almazan G (2007) Deficient peroxide detoxification underlies the susceptibility of oligodendrocyte progenitors to dopamine toxicity. Neuropharmacology 52(6):1385–1395

Hope BK (1994) A global biogeochemical budget for vanadium. Sci Total Environ 141(1–3):1–10

Hulet SW, Heyliger SO, Powers S, Connor JR (2000) Oligodendrocyte progenitor cells internalize ferritin via clathrin-dependent receptor mediated endocytosis. J Neurosci Res 61(1):52–60

Husain J, Juurlink BH (1995) Oligodendroglial precursor cell susceptibility to hypoxia is related to poor ability to cope with reactive oxygen species. Brain Res 698(1–2):86–94

Igado OO, Olopade JO, Onwuka SK, Chukwudi AC, Daramola OA, Ajufo UE (2008) Evidence of environmental pollution in caprine brains obtained from a relatively unindustrialized area in Nigeria. AJBR 11:305–309

Juurlink BH, Thorburne SK, Hertz L (1998) Peroxide-scavenging deficit underlies oligodendrocyte susceptibility to oxidative stress. Glia 22(4):371–378

Mates M (2000) Effects of antioxidant enzymes in the molecular control of reactive oxygen species toxicology. Toxicology 153:83–104

Mawatari K, Yasui Y, Sugitani K, Takadera T, Kato S (1996) Reactive oxygen species involved in the glutamate toxicity of C6 glioma cells via xc antiporter system. Neuroscience 73(1):201–208

McCarthy KD, de Vellis J (1980) Preparation of separate astroglial and oligodendroglial cell cultures from rat cerebral tissue. J Cell Biol 85(3):890–902

Monteiro HP, Winterbourn CC, Stern A (1991) Tetravalent vanadium releases ferritin iron which stimulates vanadium-dependent lipid peroxidation. Free Radic Res Commun 12–13(Pt 1):125–129

Nagaoka MH, Akiyama H, Maitani T (2004) Binding patterns of vanadium to transferrin in healthy human serum studied with HPLC/high resolution ICP-MS. Analyst 129(1):51–54

Nriagu JO, Pacyna JM (1988) Quantitative assessment of worldwide contamination of air, water and soils by trace metals. Nature 333(6169):134–139

Ray RS, Rana B, Swami B, Venu V, Chatterjee M (2006) Vanadium mediated apoptosis and cell cycle arrest in MCF7 cell line. Chem Biol Interact 163(3):239–247

Roskams AJ, Connor JR (1990) Aluminum access to the brain: a role for transferrin and its receptor. Proc Natl Acad Sci USA 87(22):9024–9027

Sabbioni E, Marafante E (1981) Relations between iron and vanadium metabolism: in vivo incorporation of vanadium into iron proteins of the rat. J Toxicol Environ Health 8(3):419–429

Sabbioni E, Rade J, Bertolero F (1980) Relationships between iron and vanadium metabolism: the exchange of vanadium between transferrin and ferritin. J Inorg Biochem 12(4):307–315

Sabbioni E, Pozzi G, Devos S, Pintar A, Casella L, Fischbach M (1993) The intensity of vanadium(V)-induced cytotoxicity and morphological transformation in BALB/3T3 cells is dependent on glutathione-mediated bioreduction to vanadium(IV). Carcinogenesis 14(12):2565–2568

Sasi MM, Haider SS, el-Fakhri M, Ghwarsha KM (1994) Microchromatographic analysis of lipids, protein, and occurrence of lipid peroxidation in various brain areas of vanadium exposed rats: a possible mechanism of vanadium neurotoxicity. Neurotoxicology 15(2):413–420

Shrivastava S (2007) Effect of tiron and its combination with nutritional supplements against vanadium intoxication in female albino rats. J Toxicol Sci 32(2):185–192

Soazo M, Garcia GB (2007) Vanadium exposure through lactation produces behavioral alterations and CNS myelin deficit in neonatal rats. Neurotoxicol Teratol 29(4):503–510

Surguladze N, Thompson KM, Beard JL, Connor JR, Fried MG (2004) Interactions and reactions of ferritin with DNA. J Biol Chem 279(15):14694–14702

Thorburne SK, Juurlink BH (1996) Low glutathione and high iron govern the susceptibility of oligodendroglial precursors to oxidative stress. J Neurochem 67(3):1014–1022

Todorich B, Zhang X, Connor JR (submitted) H-ferritin is an alternative iron delivery system to transferrin in oligodendrocytes. Glia

Todorich B, Zhang X, Slagle-Webb B, Seaman WE, Connor JR (2008) Tim-2 is the receptor for H-ferritin on oligodendrocytes. J Neurochem 107(6):1495–1505

Todorich B, Pasquini JM, Garcia CI, Paez PM, Connor JR (2009) Oligodendrocytes and myelination: the role of iron. Glia 57(5):467–478

Zhang X, Haaf M, Todorich B, Grosstephan E, Schieremberg H, Surguladze N, Connor JR (2005) Cytokine toxicity to oligodendrocyte precursors is mediated by iron. Glia 52(3):199–208